A Decentralized Approach to Generalized Power System State Estimation

Vassilis Kekatos,[1] Evangelos Vlahos,[2] Dimitris Ampeliotis,[2] Georgios B. Giannakis,[1] and Kostas Berberidis[2]
[1]Digital Tech. Center and Dept. of ECE, Univ. of Minnesota, Minneapolis, MN 55455, USA
[2]Computer Engnr. and Informatics Dept., Univ. of Patras, Rio, Patras, 26500, Greece
Emails: {vlaxose,ampeliot,berberid}@ceid.upatras.gr, {kekatos,georgios}@umn.edu

***Abstract*—Distributed generation and the urge for a more efficient grid operation will increase the frequency of network topology reconfigurations in tomorrow's power grids. High-throughput synchrophasor and intelligent electronic device readings provide unprecedented instrumentation capabilities for generalized state estimation (GSE), which deals with identifying the power system state jointly with its network topology. This task is critically challenged by the complexity scale of a grid interconnection, especially under the detailed GSE model. Upon modifying the original GSE cost by block-sparsity promoting regularizers, a decentralized solver with enhanced circuit breaker verification capabilities is developed. Built on the alternating direction method of multipliers, the novel method maintains compatibility with existing solvers and requires minimum information exchanges across the control centers of neighboring power grids. Numerical tests on an extended IEEE 14-bus model corroborate the effectiveness of the novel approach.**

I. Introduction

Network topology cognition and state estimation are two basic modules in power system monitoring [1]. For improved topology error detection, the two tasks are typically carried out jointly under the term generalized state estimation (GSE). GSE employs a detailed grid model where each substation is decomposed into its bus sections and switches, while the power system state is expanded to the bus section level and augmented by circuit breaker currents. To ensure identifiability, known breaker statuses can yield structural constraints: open (closed) switches imply zero currents (voltage drops).

The undergoing smart grid transformation brings about new challenges and opportunities for GSE. Distributed generation calls for frequent topology reconfigurations, while the control areas of an interconnection become even more strongly related in a deregulated energy market [8]. To enable situational awareness, power system states comprising thousands of variables should be securely updated in real time. At the same time, phasor measurement units (PMU) provide high-accuracy voltage and current phasors synchronized across the grid giving rise to simple linear models. Even though intelligent electronic devices (IED) can record the status of circuit breakers, not all switches are IED-instrumented, and even for the monitored ones, the reported status may be erroneous due to switch malfunctioning, communication failures, or manipulation.

Performing GSE at the interconnection level is the challenge considered here. Conventional centralized GSE solutions typically engage the least-absolute value (LAV), or the robust Huber estimators [15], [2], [13]. Alternatively, the largest normalized residual test is borrowed from bad data detection and applied in [5] on the Lagrange multipliers corresponding to circuit breaker constraints. Jointly estimating the state and the faults in DC electric circuits via ℓ_1-norm regularization has been considered in [9], where standard quadratic program solvers were employed. Reference [4] poses a mixed integer non-linear program whose complexity is not deterministically polynomial. In our recent work [12], the prior information on switches is utilized to effect block-sparsity regularizers, featuring a GSE solver with enhanced breaker status verification capabilities.

Decentralized solutions are usually confined to the conventional power system state estimator; see e.g., [6] for a recent survey. This work builds on the GSE approach in [12] and the framework of [11] to develop a decentralized GSE solver. The non-differentiability emerging with the circuit breaker verification penalties is efficiently tackled by appropriately using the alternating direction method of multipliers (ADMM) [3]. A systematic cooperation between control centers sharing state variables is enabled with unique features: backward compatibility to existing solvers, minimum inter-area exchanges, and guaranteed convergence to the centralized solution.

The rest of the paper is outlined as follows: Given phasor measurements, GSE is first modeled as an ℓ_2-norm regularized linearly-constrained quadratic program in Section II. In Section III, the novel decentralized GSE approach is developed, and it is later numerically evaluated in Section IV.

Notation: Complex-valued variables are indicated by a tilde. Lower- (upper-)case boldface letters denote column vectors (matrices), and calligraphic letters stand for sets. The notation $(\cdot)'$ denotes transposition.

II. System Modeling & Problem Statement

Consider a power interconnection partitioned into K areas, each one monitored by its own control center; see e.g., Fig. 1. The grid is modeled at the bus section/switching device network level [1, Ch. 8]. Each area k consists of B_k bus sections, called simply buses hereafter, L_k transmission lines, and C_k circuit breakers. Let $\tilde{\mathbf{v}}_k \in \mathbb{C}^{B_k}$, $\tilde{\mathbf{i}}_k \in \mathbb{C}^{B_k}$, $\tilde{\mathbf{f}}_k \in \mathbb{C}^{L_k}$, and $\tilde{\mathbf{s}}_k \in \mathbb{C}^{C_k}$ denote the vectors of bus voltages, current injections, line currents, and breaker currents, respectively. By convention, current directionality is from lower- to higher-indexed buses.

If $\tilde{\mathbf{Y}}_{f,k}$ is the area k's line-bus admittance matrix, Ohm's law implies

$$\tilde{\mathbf{f}}_k = \tilde{\mathbf{Y}}_{f,k}\tilde{\mathbf{v}}_k. \quad (1)$$

Work in this paper was supported by the Institute of Renewable Energy and the Environment (IREE) under grant no. RL-0010-13, Univ. of Minnesota.

978-1-4673-3146-3/13/$31.00 ©2013IEEE

To model the effect of area k's breakers, define the $C_k \times B_k$ breaker-bus incidence matrix $\mathbf{A}_k$: if the c-th breaker connects buses m and n in area k, the $m(n)$-th entry of the c-th row of $\mathbf{A}_k$ is equal to $+1(-1)$, and zero otherwise. Kirchoff's current law asserts that the sum of the currents flowing out of every bus is zero, or

$$\tilde{\mathbf{i}}_k = \tilde{\mathbf{Y}}_k \tilde{\mathbf{v}}_k + \mathbf{A}_k' \tilde{\mathbf{s}}_k \tag{2}$$

where $\tilde{\mathbf{Y}}_k$ is the bus admittance matrix of area k [6].

Power systems are currently being instrumented with phasor measurement units that can measure voltage and current phasors across the grid. Moreover, if an intelligent electronic device has been installed on a circuit breaker, the breaker status (open or closed) is reported to the control center. However, not all entries of $(\tilde{\mathbf{v}}_k, \tilde{\mathbf{i}}_k, \tilde{\mathbf{f}}_k, \tilde{\mathbf{s}}_k)$ are measured, and not all breakers are monitored either. Given the area grid model [cf. (1)-(2)], together with the analog measurements and the reported breaker statutes collected in that area; the generalized state estimator (GSE) aims at jointly estimating the area system state and determining the status of unmonitored breakers.

Specifically, the power system state in GSE is augmented from $\tilde{\mathbf{v}}_k$ to include $\tilde{\mathbf{s}}_k$ too. According to (1)-(2), the measured entries of $(\tilde{\mathbf{v}}_k, \tilde{\mathbf{i}}_k, \tilde{\mathbf{f}}_k, \tilde{\mathbf{s}}_k)$ are linearly related to the augmented state $\tilde{\mathbf{x}}_k := [\tilde{\mathbf{v}}_k' \ \tilde{\mathbf{s}}_k']'$. Upon expressing both PMU measurements $\tilde{\mathbf{z}}_k$ and states $\tilde{\mathbf{x}}_k$ in rectangular coordinates, the following real-valued measurement model holds:

$$\mathbf{z}_k = \mathbf{H}_k \mathbf{x}_k + \mathbf{n}_k \tag{3}$$

where $\mathbf{z}_k := [\mathrm{Re}\{\tilde{\mathbf{z}}_k\}' \ \mathrm{Im}\{\tilde{\mathbf{z}}_k\}']' \in \mathbb{R}^{M_k}$; $\mathbf{H}_k$ is the associated measurement matrix; $\mathbf{x}_k := [\mathrm{Re}\{\tilde{\mathbf{x}}_k\}' \ \mathrm{Im}\{\tilde{\mathbf{x}}_k\}']' \in \mathbb{R}^{N_k}$ for $N_k := 2(B_k + C_k)$; while $\mathbf{n}_k$ captures instrumentation errors and modeling inaccuracies modeled as a zero-mean random vector whose covariance is the identity matrix.

Although each measurement is collected by a single control center, neighboring areas may have shared state variables resulting in partially overlapping $\mathbf{x}_k$'s. In the toy interconnection of Fig. 1 for example, area 1 measures the current flowing on line 37-44. Even though the voltage at bus 44 is not in the footprint of area 1, it is included in state vector $\mathbf{x}_1$ since it is related to the aforementioned 37-44 line current reading.

The measurements described by (3) typically do not suffice to ensure identifiability of the augmented state $\mathbf{x}_k$. GSE alleviates this concern by further imposing network topology-implied constraints. In detail, if no load or generation resides at a bus, its bus injection current is always zero; and that is the case for the majority of the buses in Fig. 1 – except for those indicated by arrows such as bus 15. It is then obvious from (2) that every zero-injection bus incurs two real-valued linear constraints on $\mathbf{x}_k$. Additional nullspace constraints are dictated by breaker statuses. When a breaker is open, its current is apparently zero; whereas, if closed, the voltage drop across its ends is zero (recall that a breaker has zero-impedance). To form the constraints, let $\mathbf{e}_m$ be the m-th canonical vector. If breaker m of area k is open, then $\mathbf{e}_m' \tilde{\mathbf{s}}_k = 0$; otherwise, $\mathbf{e}_m' \mathbf{A}_k \tilde{\mathbf{v}}_k = 0$. Hence, every monitored breaker status contributes a pair of linear constraints on $\mathbf{x}_k$.

Upon expressing all T_k topology-imposed constraints as $\mathbf{C}_k \mathbf{x}_k = \mathbf{0}$, finding the GSE for area k can be then posed as the linearly-constrained least-squares problem

$$\hat{\mathbf{x}}_{k,\mathrm{LSE}} := \arg\min_{\mathbf{x}_k} \ \frac{1}{2}\|\mathbf{z}_k - \mathbf{H}_k \mathbf{x}_k\|_2^2 \quad \text{s.t.} \ \ \mathbf{C}_k \mathbf{x}_k = \mathbf{0}. \tag{4}$$

Albeit the GSE in (4) can be found in closed form, it has several limitations. First, prior information on uninstrumented breakers, such as typical substation configurations, is not accounted for. Even for a monitored breaker, there could be reasonable concerns (e.g., large measurement residuals) in using its recorded status as a hard constraint. Furthermore, inferring the status of an unmonitored breaker m could be misleading, since the $(\hat{\tilde{\mathbf{s}}}_{k,\mathrm{LSE}}, \hat{\tilde{\mathbf{v}}}_{k,\mathrm{LSE}})$ corresponding to $\hat{\mathbf{x}}_{k,\mathrm{LSE}}$ will yield neither $\mathbf{e}_m' \hat{\tilde{\mathbf{s}}}_{k,\mathrm{LSE}} = 0$, nor $\mathbf{e}_m' \mathbf{A}_k \hat{\tilde{\mathbf{v}}}_{k,\mathrm{LSE}} = 0$. Finally, solving separately the K GSE problems of (4) is suboptimal due to the variable sharing, and the risk of compromising local observability.

To tackle the limitations associated with uninstrumented or suspected circuit breakers, a block-sparsity-promoting GSE approach was proposed in [12]. Let $\mathcal{B}_k$ be the set of all breakers whose status must be verified in area k. If breaker $m \in \mathcal{B}_k$ is suspected to be open, then the vector $[\mathrm{Re}\{\mathbf{e}_m' \tilde{\mathbf{s}}_k\} \ \mathrm{Im}\{\mathbf{e}_m' \tilde{\mathbf{s}}_k\}]'$ is zero. Alternatively, if breaker m is expected to be closed, the vector $[\mathrm{Re}\{\mathbf{e}_m' \mathbf{A} \tilde{\mathbf{v}}_k\} \ \mathrm{Im}\{\mathbf{e}_m' \mathbf{A} \tilde{\mathbf{v}}_k\}]'$ will be zero instead. Either way, prior information on breaker m incurs block sparsity on the vector $\mathbf{B}_{k,m} \mathbf{x}_k$ for an appropriately defined $2 \times N_k$ matrix $\mathbf{B}_{k,m}$. Penalizing the cost in (4) by the number of nonzero $\{\mathbf{B}_{k,m} \mathbf{x}_k\}_{m \in \mathcal{B}_k}$ leads to a hard optimization problem. Motivated by advances in block-compressed sensing, the latter problem was finally relaxed to the second-order cone program

$$\min_{\mathbf{x}_k} \ \frac{1}{2}\|\mathbf{z}_k - \mathbf{H}_k \mathbf{x}_k\|_2^2 + \lambda \sum_{m \in \mathcal{B}_k} \|\mathbf{B}_{k,m} \mathbf{x}_k\|_2 \quad \text{s.t.} \ \ \mathbf{C}_k \mathbf{x}_k = \mathbf{0} \tag{5}$$

where $\lambda > 0$ is a tuning parameter.

III. A Decentralized Algorithm

Solving each per area GSE of (5) separately is clearly suboptimal. Indeed, measurements are used only by the control center they are collected at shared state estimates will not agree, while control areas may become unidentifiable. An interconnection-wide GSE should consider minimizing the sum of the per area costs subject to the per-area constraints in (5), yet critically ensure inter-area consensus on shared states. Such a goal can be achieved via solving

$$\min_{\{\mathbf{x}_k\}} \ \sum_{k=1}^{K} \left(\frac{1}{2}\|\mathbf{z}_k - \mathbf{H}_k \mathbf{x}_k\|_2^2 + \lambda \sum_{m \in \mathcal{B}_k} \|\mathbf{B}_{k,m} \mathbf{x}_k\|_2 \right) \tag{6a}$$

$$\text{s.t.} \ \ \mathbf{C}_k \mathbf{x}_k = \mathbf{0}, \qquad \forall \ k \tag{6b}$$

$$\mathbf{x}_k[l] = \mathbf{x}_l[k], \quad \forall \ l \in \mathcal{N}_k, \forall \ k \tag{6c}$$

where $\mathcal{N}_k$ is the set of areas sharing states with area k, and $\mathbf{x}_k[l]$ denotes the subvector of $\mathbf{x}_k$ containing the state variables shared with area $l \in \mathcal{N}_k$.

Towards a decentralized algorithm for solving (6), the consensus constraints in (6c) should be decoupled across areas. That can be accomplished upon introducing auxiliary variables $\mathbf{x}_{kl}$, and replacing (6c) by the pair of constraints $\mathbf{x}_k[l] = \mathbf{x}_{kl}$

and $\mathbf{x}_l[k] = \mathbf{x}_{kl}$. Moreover, to effectively cope with the nondifferentiability of the $\|\mathbf{B}_{k,m}\mathbf{x}_k\|_2$ terms in (6a), additional auxiliary variables $\mathbf{u}_{k,m} = \mathbf{B}_{k,m}\mathbf{x}_k$ are introduced as

$$\min_{\substack{\{\mathbf{x}_k,\mathbf{x}_{kl}\}\\ \{\mathbf{u}_{k,m}\}}} \sum_{k=1}^{K}\left(\frac{1}{2}\|\mathbf{z}_k-\mathbf{H}_k\mathbf{x}_k\|_2^2+\lambda\sum_{m\in\mathcal{B}_k}\|\mathbf{u}_{k,m}\|_2\right) \quad (7a)$$

$$\text{s.t.}\quad \mathbf{C}_k\mathbf{x}_k=\mathbf{0},\quad \forall\, k \quad (7b)$$

$$\mathbf{u}_{k,m}=\mathbf{B}_{k,m}\mathbf{x}_k,\quad \forall\, m\in\mathcal{B}_k,\ \forall\, k \quad (7c)$$

$$\mathbf{x}_k[l]=\mathbf{x}_{kl},\quad \forall\, l\in\mathcal{N}_k,\ \forall k. \quad (7d)$$

Optimization in (7) is subsequently solved using ADMM, a method that has been applied for distributing several optimization problems [14], [3]. Lagrange multipliers $\{\boldsymbol{\mu}_{k,m}\}_{m\in\mathcal{B}_k,k}$ and $\{\boldsymbol{\nu}_{kl}\}_{k,l}$ are first introduced for constraints (7c) and (7d), respectively. ADMM then exploits the method of multipliers concatenated with an iteration of the Gauss-Seidel algorithm. After defining the augmented Lagrangian function of (7) as

$$L_c\left(\{\mathbf{x}_k,\mathbf{u}_{k,m},\mathbf{x}_{kl}\};\{\boldsymbol{\mu}_{k,m}\boldsymbol{\nu}_{kl}\}\right):= \quad (8)$$

$$\sum_{k=1}^{K}\Bigg(\frac{1}{2}\|\mathbf{z}_k-\mathbf{H}_k\mathbf{x}_k\|_2^2+\lambda\sum_{m\in\mathcal{B}_k}\|\mathbf{u}_{k,m}\|_2$$

$$+\sum_{m\in\mathcal{B}_k}\left(\boldsymbol{\mu}'_{k,m}(\mathbf{u}_{k,m}-\mathbf{B}_{k,m}\mathbf{x}_k)+\frac{c}{2}\|\mathbf{u}_{k,m}-\mathbf{B}_{k,m}\mathbf{x}_k\|_2^2\right)$$

$$+\sum_{l\in\mathcal{N}_k}\left(\boldsymbol{\nu}'_{kl}(\mathbf{x}_k[l]-\mathbf{x}_{kl})+\frac{c}{2}\|\mathbf{x}_k[l]-\mathbf{x}_{kl}\|_2^2\right)\Bigg)$$

for a predefined constant $c>0$, ADMM iterates through the following steps:

$$\{\mathbf{x}_k^{t+1}\}=\arg\min_{\{\mathbf{C}_k\mathbf{x}_k=\mathbf{0}\}} L_c(\{\mathbf{x}_k,\mathbf{u}_{k,m}^t,\mathbf{x}_{kl}^t\};\{\boldsymbol{\mu}_{k,m}^t\boldsymbol{\nu}_{kl}^t\}) \quad (9a)$$

$$\{\mathbf{x}_{kl}^{t+1},\mathbf{u}_{k,m}^{t+1}\}=\arg\min_{\substack{\{\mathbf{x}_{kl}\},\\ \{\mathbf{u}_{k,m}\}}} L_c(\{\mathbf{x}_k^{t+1},\mathbf{u}_{k,m},\mathbf{x}_{kl}\};\{\boldsymbol{\mu}_{k,m}^t\boldsymbol{\nu}_{kl}^t\}) \quad (9b)$$

$$\boldsymbol{\mu}_{k,m}^{t+1}=\boldsymbol{\mu}_{k,m}^t+c\cdot(\mathbf{u}_{k,m}^{t+1}-\mathbf{B}_{k,m}\mathbf{x}_k^{t+1}),\quad \forall m\in\mathcal{B}_k,\ \forall k \quad (9c)$$

$$\boldsymbol{\nu}_{kl}^{t+1}=\boldsymbol{\nu}_{kl}^t+c\cdot(\mathbf{x}_k^{t+1}[l]-\mathbf{x}_{kl}^{t+1})\quad \forall k,l \quad (9d)$$

which are elaborated next.

Starting with the update of $\mathbf{x}_k$'s, notice that the minimization in (9a) decouples across areas. Assuming that $\{\mathbf{u}_{k,m}^t,\boldsymbol{\mu}_{k,m}^t\}_{m\in\mathcal{B}_k}$ and $\{\mathbf{x}_{kl}^t,\boldsymbol{\nu}_{kl}^t\}_{l\in\mathcal{N}_k}$ are available at the k-th control center, the local state iterate $\mathbf{x}_k^{t+1}$ can be updated in closed form as the minimizer of a linearly-constrained convex quadratic program. Actually, it will be shown shortly that the auxiliary variables $\{\mathbf{x}_{kl}^t\}_{l\in\mathcal{N}_k}$ can be eliminated.

Since the augmented Lagrangian is separable with respect to $\{\mathbf{u}_{k,m}\}$ and $\{\mathbf{x}_{kl}\}$, the minimization of (9b) decouples over the two variable sets. Then, it can be verified that $\mathbf{x}_{kl}$'s are updated as

$$\mathbf{x}_{kl}^{t+1}=\frac{\mathbf{x}_k^{t+1}[l]+\mathbf{x}_l^{t+1}[k]}{2}+\frac{\boldsymbol{\nu}_{kl}^t+\boldsymbol{\nu}_{lk}^t}{2c}. \quad (10)$$

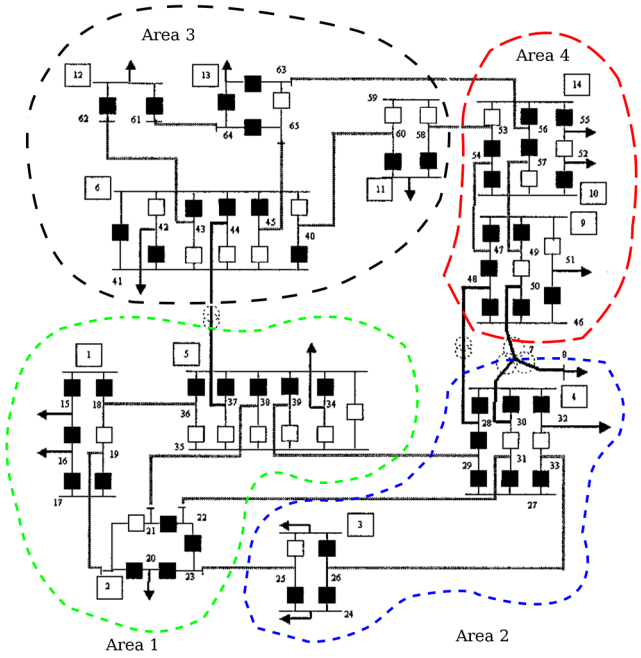

Fig. 1: The IEEE 14-bus system modeled at the substation level [7]. Solid (hollow) squares indicate closed (open) circuit breakers, and thick (thin) lines correspond to transmission lines (breaker connections). Lassos show control area footprints.

Consider next the updates of $\boldsymbol{\nu}_{kl}$ and $\boldsymbol{\nu}_{lk}$ according to (9d). As in [11] and [14], adding the two updates by parts and solving for $\mathbf{x}_{kl}^{t+1}$ yields

$$\mathbf{x}_{kl}^{t+1}=\frac{\mathbf{x}_k^{t+1}[l]+\mathbf{x}_l^{t+1}[k]}{2}+\frac{\boldsymbol{\nu}_{kl}^t+\boldsymbol{\nu}_{lk}^t}{2c}-\frac{\boldsymbol{\nu}_{kl}^{t+1}+\boldsymbol{\nu}_{lk}^{t+1}}{2c}. \quad (11)$$

By equating the right-hand sides of (10) and (11), yields $\boldsymbol{\nu}_{kl}^t+\boldsymbol{\nu}_{lk}^t=\mathbf{0}$ for all t. Thus, the second summand in (10) is cancelled, and the iterate $\mathbf{x}_{kl}^t$ can be merely substituted by the mean of $\mathbf{x}_k^t[l]$ and $\mathbf{x}_l^t[k]$ in all other updates.

Regarding the $\{\mathbf{u}_{k,m}\}$ variables, the minimization in (9b) decouples not only across areas, but over the single $\{\mathbf{u}_{k,m}\}_{m\in\mathcal{B}_k}$ too. After completing the squares, the latter can be updated by solving

$$\mathbf{u}_{k,m}^{t+1}:=\arg\min_{\mathbf{u}_{k,m}}\ \lambda\|\mathbf{u}_{k,m}\|_2+\frac{c}{2}\|\mathbf{u}_{k,m}-\mathbf{d}_{k,m}^{t+1}\|_2^2 \quad (12)$$

where $\mathbf{d}_{k,m}^{t+1}:=\mathbf{B}_{k,m}\mathbf{x}_k^{t+1}-\frac{1}{c}\boldsymbol{\mu}_{k,m}^t$. Interestingly, using the notion of the subdifferential, the minimizer of (12) is provided in closed form as (see e.g., [10, Sec. V.B])

$$\mathbf{u}_{k,m}^{t+1}=\mathbf{d}_{k,m}^{t+1}\cdot\left[1-\frac{\lambda}{c\cdot\|\mathbf{d}_{k,m}^{t+1}\|_2}\right]_+ \quad (13)$$

where $[x]_+:=\max\{x,0\}$. The block-thresholding operator in (13) indicates that depending on the value of λ, the iterates $\mathbf{u}_{k,m}^t$ will be block-sparse, and thus most of the $\mathbf{B}_{k,m}\mathbf{x}_k^t$ vectors will be driven to zero as desired.

An iteration cycle ends with the steps (9c)-(9d). Using again the simplification of (10), (9d) boils down to

$$\boldsymbol{\nu}_{kl}^{t+1}=\boldsymbol{\nu}_{kl}^t+c\cdot\frac{\mathbf{x}_k^{t+1}[l]-\mathbf{x}_l^{t+1}[k]}{2}. \quad (14)$$

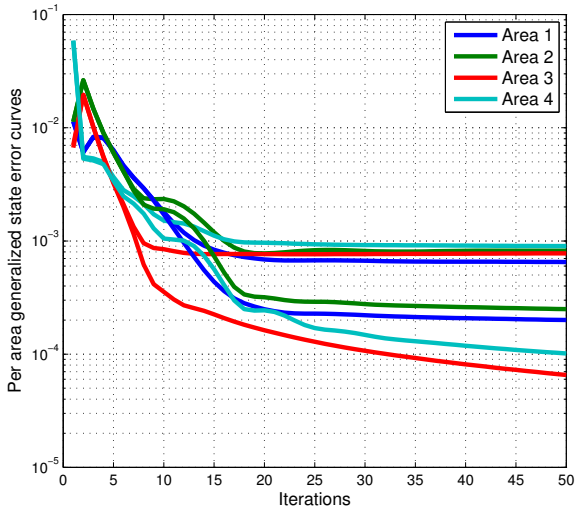

Fig. 2: Per area error curves $e^t_{k,c}$ (bottom) and $e^t_{k,o}$ (top) for the novel decentralized GSE algorithm.

IV. Numerical Tests

The derived decentralized GSE is numerically evaluated using the IEEE 14-bus benchmark system depicted in Fig. 1 [7]. Power system measurements and admittance matrices were generated by the MATLAB toolbox MATPOWER [16]. The interconnection-wide state comprises 65 bus voltages and 73 circuit breaker currents, and 316 measurements are collected. Among all 65 buses, bus voltages phasors are recorded only at the 30 buses indicated by either boxed numbers, the bus-bar symbol, or the injection symbol; e.g. buses 1, 17, and 15, respectively. Injection currents are metered at the 15 injection buses, and line currents are measured on both ends of all transmission lines. Finally, IEDs record the current flow on all 73 breakers. Measurement noise is modeled as Gaussian with standard deviation per real component $\sigma_V = 0.01$ and $\sigma_I = 0.02$ for voltages and currents, respectively.

To evaluate the convergence of the algorithm, two performance metrics are adopted: the per area error to the centralized solution of (6), that is $e^t_{k,c} := \|\mathbf{x}^{(c)}_k - \mathbf{x}^t_k\|_2/N_k$, and the per area error to the true state defined as $e^t_{k,o} := \|\mathbf{x}_k - \mathbf{x}^t_k\|_2/N_k$. Parameter c is set to 10^{-4}, even though, empirically, the algorithm was not sensitive to its selection. The obtained error curves shown in Fig. 2 indicate that the decentralized algorithm achieves the estimation accuracy of the centralized one within a few iterations.

The circuit breaker verification capabilities of the new approach were considered next. A subset of suspected breakers $\mathcal{S}$ was sampled uniformly at random from $\{1, \ldots, 73\}$. In 80% of the breakers in $\mathcal{S}$, the assumed status coincided with the true one, whereas for the rest 20% it was reversed. Figure 3 shows the number of breaker status errors obtained by the ordinary GSE [cf. (6) with $\lambda = 0$] and the decentralized ℓ_2-regularized GSE of (7) with $\lambda = 10^3$, for subsets $\mathcal{S}$ of increasing cardinality and averaged over 100 Monte Carlo experiments. The numerical results corroborate the enhanced breaker status verification properties of the novel approach.

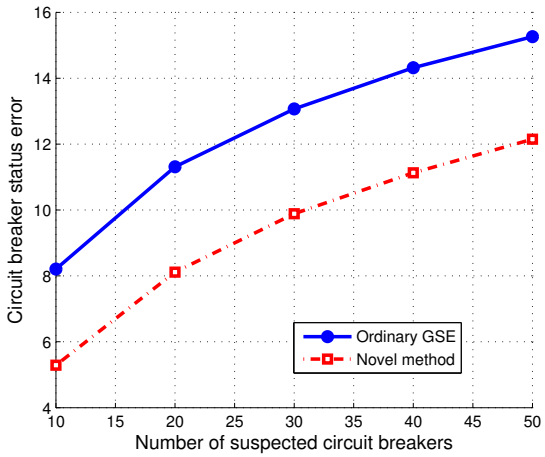

Fig. 3: Circuit breaker status errors.

References

[1] A. Abur and A. Gómez-Expósito, *Power System State Estimation: Theory and Implementation*. New York, NY: Marcel Dekker, 2004.

[2] A. Abur, H. Kim, and M. Celik, "Identifying the unknown circuit breaker statuses in power networks," *IEEE Trans. Power Syst.*, vol. 10, no. 4, pp. 2029–2035, Nov. 1995.

[3] S. Boyd, N. Parikh, E. Chu, B. Peleato, and J. Eckstein, "Distributed optimization and statistical learning via the alternating direction method of multipliers," *Found. Trends Mach Learning*, vol. 3, pp. 1–122, 2010.

[4] E. Caro, A. Conejo, and A. Abur, "Breaker status identification," *IEEE Trans. Power Syst.*, vol. 25, no. 2, pp. 694–702, May 2010.

[5] K. A. Clements and A. S. Costa, "Topology error identification using normalized Lagrange multipliers," *IEEE Trans. Power Syst.*, vol. 13, no. 2, pp. 347–353, May 1998.

[6] G. B. Giannakis, V. Kekatos, N. Gatsis, S.-J. Kim, H. Zhu, and B. F. Wollenberg, "Monitoring and optimization for power grids: A signal processing perspective," (Sep. 2013).

[7] A. Gómez-Expósito and A. de la Villa Jaén, "Reduced substation models for generalized state estimation," *IEEE Trans. Power Syst.*, vol. 16, no. 4, pp. 839–846, Nov. 2001.

[8] A. Gómez-Expósito, A. Abur, A. de la Villa Jaén, and C. Gómez-Quiles, "A multilevel state estimation paradigm for smart grids," *Proc. IEEE*, vol. 99, no. 6, pp. 952–976, Jun. 2011.

[9] D. Gorinevsky, S. Boyd, and S. Poll, "Estimation of faults in DC electrical power system," in *Proc. IEEE Conf. on Decision and Control*, Shanghai, China, Dec. 2009, pp. 4334–4339.

[10] V. Kekatos and G. B. Giannakis, "From sparse signals to sparse residuals for robust sensing," *IEEE Trans. Signal Process.*, vol. 59, no. 7, pp. 3355–3368, Jul. 2011.

[11] ——, "Distributed robust power system state estimation," *IEEE Trans. Power Syst.*, vol. 28, no. 2, pp. 1617–1626, Feb. 2013.

[12] ——, "Joint power system state estimation and breaker status identification," in *Proc. North American Power Symposium*, University of Illinois, Urbana-Champaign, IL, Sep. 2012.

[13] L. Mili, G. Steeno, F. Dobraca, and D. French, "A robust estimation method for topology error identification," *IEEE Trans. Power Syst.*, vol. 14, no. 4, pp. 1469–1476, Nov. 1999.

[14] I. D. Schizas, A. Ribeiro, and G. B. Giannakis, "Consensus in ad hoc WSNs with noisy links - Part I: Distributed estimation of deterministic signals," *IEEE Trans. Signal Process.*, vol. 56, no. 1, pp. 350–364, Jan. 2008.

[15] H. Singh and F. L. Alvarado, "Network topology determination using least absolute value state estimation," *IEEE Trans. Power Syst.*, vol. 10, no. 3, pp. 1159–1165, Aug. 1995.

[16] R. D. Zimmerman, C. E. Murillo-Sanchez, and R. J. Thomas, "MATPOWER: steady-state operations, planning and analysis tools for power systems research and education," *IEEE Trans. Power Syst.*, vol. 26, no. 1, pp. 12–19, Feb. 2011.